Proceedings of the ASME 2009 Heat Transfer Summer Conference
HT2009
July 19-23, 2009, San Francisco, California USA

HT2009-88029

THERMAL CONDUCTIVITY OF WATER/CARBON NANOTUBE COMPOSITE SYSTEMS: INSIGHTS FROM MOLECULAR DYNAMICS SIMULATIONS

J. A. Thomas, R. M. Iutzi, and A. J. H. McGaughey*
Department of Mechanical Engineering
Carnegie Mellon University
Pittsburgh, Pennsylvania 15213
Email: jathomas@cmu.edu, iutzi@cmu.edu, mcgaughey@cmu.edu

ABSTRACT

The effective thermal conductivity of water/carbon nanotube (CNT) composite systems is predicted using molecular dynamics simulation. Both empty and water-filled CNTs with diameters ranging from 0.83 nm to 1.26 nm are considered. Using a direct application of the Fourier law, we explore the transition to diffusive phonon transport with increasing CNT length and identify the correlation between CNT diameter and fully-diffusive thermal conductivity. Using Green-Kubo linear response theory, we explore how the thermal conductivity of water inside CNT varies with tube diameter. We predict the effective thermal conductivity of the composite systems and examine how the phonon modes in the CNT are affected by interactions with the water molecules.

INTRODUCTION

Due to their high thermal conductivities, graphene sheets and carbon nanotubes (CNT) are ideal candidates for next-generation thermal management devices [1]. Most experimental and theoretical investigations of thermal transport in these materials, however, have focused on their behavior in a vacuum. As components of a thermal management device, the atoms in CNTs and graphene sheets will exchange energy with atoms and molecules in an adjacent solid, liquid, or gas. Understanding how such interactions with non-bonded atoms modify thermal transport is an important next step in predicting how these materials will behave in heat transfer applications.

The high thermal conductivity of graphitic structures is attributed to their rigid crystalline structure and resulting long phonon mean free paths [2]. In CNTs and graphene sheets shorter than about 100 nm, thermal energy is transported diffusely by phonons that scatter inside the system and ballistically by phonons that scatter with the system boundaries. With increasing system size, longer wavelength vibrational modes that can travel ballistically through the system are accessed and the thermal conductivity off the system increases [2, 3]. In systems longer than about 1 μm, however, the contribution to the thermal conductivity from these long-wavelength ballistic modes becomes negligible, most modes become diffusive, and the thermal conductivity becomes independent of the CNT length [4]. Information concerning how this transition length varies with CNT diameter and interactions with an adjacent material is not yet available.

In this work we use molecular dynamics (MD) simulation to investigate the thermal conductivity of CNTs filled with water, a common coolant and well-characterized fluid. We begin by describing our simulation procedure. Next, we investigate the variation in CNT thermal conductivity with diameter and length for hollow CNTs and explore the transition to fully diffusive phonon transport. We then predict the thermal conductivity of water confined inside CNTs and examine how changes in the water structure with CNT diameter modify the CNT thermal conductivity. We finish by examining the thermal conductivity of water/CNT composite systems.

*Address all correspondence to this author.

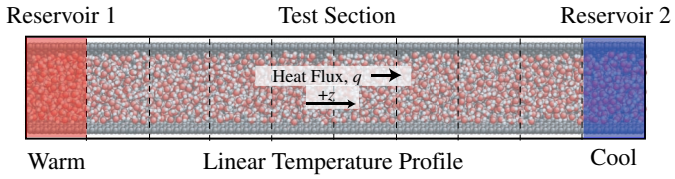

Figure 1. TYPICAL WATER/CNT COMPOSITE WITH IMPOSED HEAT FLUX. WE CALCULATE THE TEMPERATURE GRADIENT BY PREDICTING THE TEMPERATURE WITHIN BINS (DASHED LINES) ALONG THE TUBE AXIS AND PERFORMING A LINEAR REGRESSION.

SIMULATION SET-UP

The small length and time scales associated with atomic-level dynamics limit the ability of laboratory experiments to resolve nanoscale transport phenomena. Instead, MD simulation, which can access these scales, has become a common tool for modeling atomistic transport. Molecular dynamics is a simulation technique that uses Newton's laws of motion to predict the position and momenta space trajectories of a system of classical particles. The only required inputs are an interatomic potential, which is used to calculate potential energies and forces, and an initial atomic configuration.

We examine empty and water-filled 0.83, 1.10, and 1.26 nm diameter CNTs [with chirality vectors of (6,6), (8,8) and (10,10)] with lengths ranging from 200 nm to 1200 nm. Interactions between carbon atoms are modeled using the second-generation REBO potential developed by Brenner *et al* [5]. The REBO potential is a classical potential function that models atomic interactions by describing changes in the atomic orbital hybridization due to the breaking and forming of covalent bonds. The REBO potential function reproduces the known bond energies and bond lengths for a variety of hydrocarbon structures. For graphitic structures, where each atom remains bonded to three nearest-neighbor atoms, the REBO potential can be implemented to scale linearly with the number of carbon atoms in the system.

Interactions between water molecules are modeled using the TIP4P/2005 potential [6]. The TIP4P/2005 water model is a pair potential that describes interactions between water molecules using a Lennard-Jones (LJ) potential between oxygen atoms and Columbic interactions between charged interaction sites located on each water molecule. The magnitude of the charges, the positions of the charged interaction sites, and the LJ potential parameters used in the potential were tuned to reproduce the experimentally-observed bulk-water radial distribution function, the variation in water density with temperature, and other thermophysical properties. We model water/carbon interactions using the LJ potential of Werder *et al.* where the oxygen atoms interact directly with the carbon atoms on the CNT surface [7]. The parameters of the LJ potential are tuned to reproduce the experimentally observed water/graphene contact angle.

From the intermolecular potential function, we can evaluate the intermolecular forces and calculate the kinematic trajectories of the molecules. We integrate the equations of motion using a velocity Verlet scheme with a 1.0 fs time step. We model the rotational dynamics of the water molecules using the quaternion method [8]. The total energy of the simulation during data collection is constant and the average simulation temperature is 298 K.

The number of carbon atoms in the CNT ranges from 29,232 (for the 200 nm long, 0.83 nm-diameter CNT) to 194,880 (for the 1200 nm long, 1.26 nm-diameter CNT). To predict the equilibrium water density inside the CNTs, we simulated an open-ended sample of each nanotube interacting with a water reservoir at a temperature and pressure of 298 K and 1 atm. The density of the water in the reservoir was maintained at 1000 kg/m^3 and water molecules were able to freely diffuse across the open ends of the tube. After 250 ps, the average number of molecules enclosed in the tube became steady, allowing us to determine the equilibrium density [9]. Depending on the tube diameter, as discussed in our previous work, the liquid density inside the CNT may be less than 1000 kg/m^3 and the liquid structure may be different from that of bulk water [10, 11]. The CNTs used to generate all of the subsequently reported data span the entire simulation cell and (for simulations involving filled CNTs) were initially filled with the number of molecules corresponding to this equilibrium density.

THERMAL CONDUCTIVITY OF HOLLOW CNTs

We predict the axial thermal conductivity, k_z, of hollow CNTs using the Fourier Law:

$$q_z = -k_z A_c \frac{dT}{dz}, \tag{1}$$

where q_z is the heat flow in the z-direction (see Fig. 1), A_c is the CNT cross sectional area, and dT/dz is the axial temperature gradient. We introduce a heat flux by transferring a known quantity of kinetic energy from Reservoir 2 to Reservoir 1 at each time step [12]. This energy redistribution procedure does not change the total system energy and does not affect the total system momentum. In response to this energy redistribution, however, thermal energy moves from Reservoir 1 to Reservoir 2 and a temperature gradient is established along the CNT axis. By controlling the heat flux through the CNT, we can calculate the CNT thermal conductivity from the axial temperature gradient. We fix the carbon atoms at the edge of the tube to ensure that all of the transferred energy passes through the test section and to prevent carbon atom sublimation.

For the hollow CNTs, the heat flow through the CNT is between 30 nW and 50 nW and the induced temperature gradient is between 7 K/μm and 20 K/μm. Remaining consistent with previous reports, we define the cross-sectional area of the CNT to

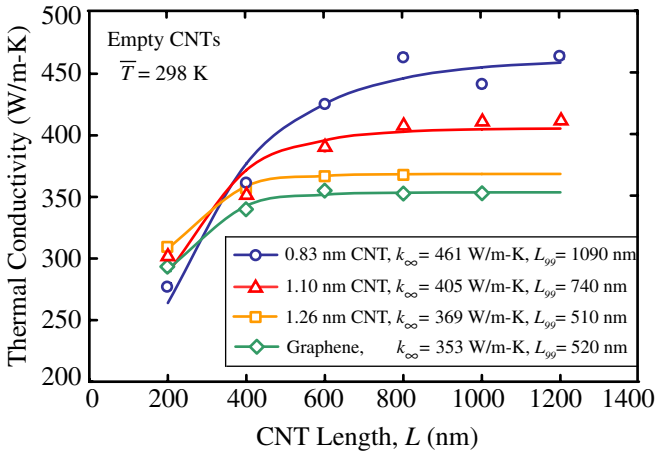

Figure 2. VARIATION IN CNT THERMAL CONDUCTIVITY WITH LENGTH.

be $A_c(d) = \pi \times d \times b$, where b = 0.34 nm is the van der Waals "thickness" of the CNT surface and d is the CNT diameter [4,13].

In Fig. 2, we present the variation in thermal conductivity with length and diameter for 0.83, 1.10, and 1.25 nm diameter CNTs. Each simulation consists of a 5 ns equilibration period, followed by a 5 ns to 10 ns data collection period. From this thermal conductivity data, we can observe the transition from a regime where the CNT thermal conductivity is length-dependent $[k_z = k_z(d,L)]$ to a regime where the thermal conductivity is independent of the tube length and phonon transport is fully diffusive $[k_z = k_z(d)]$. To quantify this transition, we fit the simulation data to the empirical function:

$$k = k_\infty \left[1 - \exp\left(-\frac{L}{L_c}\right)\right], \tag{2}$$

where k_∞ is the fully-diffusive thermal conductivity, L is the sample length, and L_c is a decay constant that describes the transition rate from ballistic to diffusive transport. We define the quantity L_{99} to be the length at which $k = 0.99k_\infty$, such that

$$L_{99} = \ln(100) \cdot L_c. \tag{3}$$

We find that L_{99} and k_∞, included in Fig. 2, increase with decreasing CNT diameter. This result is consistent with the MD simulations of Shiomi and Maruyama, who predict that the thermal conductivity in the diffusive regime of a 0.64 nm diameter CNT is larger than that of a 0.75 nm diameter CNT [4]. For the graphene sheet, which is periodic in two directions and representative of an infinite-diameter CNT, the thermal conductivity is 353 W/m-K. We find that increasing the width of the graphene sample beyond the 5 nm width used here has no detectable affect on the predicted thermal conductivity. Consistent with data from other reports, we find that the thermal conductivities of graphite systems predicted using the REBO potential is lower than those measured from experiments [13].

THERMAL CONDUCTIVITY OF WATER INSIDE CNTs

The next step in predicting the thermal transport properties of water/CNT composite systems is to explore the thermal conductivity of water confined inside CNTs. Due to confinement-related changes in the liquid structure [9, 11], we expect that the thermal conductivity of water inside the CNT will vary with CNT diameter. We can predict the thermal conductivity of water by inducing a heat flux and measuring the resulting temperature gradient or by performing equilibrium simulations using Green-Kubo linear response theory. We use the Green-Kubo method, which allows us to examine the energy exchange mechanisms that contribute to the liquid thermal conductivity (see below). We keep the carbon atoms fixed in space to eliminate thermal energy exchange with the CNT. The effect of fixing the carbon atoms on the dynamics and thermophysical properties of the water molecules is discussed below.

For water, the heat flux vector is defined by [14],

$$\mathbf{J}(t) = \sum_i \mathbf{v_i} e_i - \frac{1}{2}\sum_i \sum_j \mathbf{r_{ij}} \left(\mathbf{v_i} \cdot \mathbf{F_{ij}} + \boldsymbol{\omega}_{\mathbf{pi}} \cdot \boldsymbol{\tau}_{\mathbf{pi}}\right), \tag{4}$$

where $\mathbf{v_i}$ and e_i are the velocity vector and potential energy of molecule i, $\mathbf{r_{ij}}$ is the position vector from molecule i to molecule j, $\boldsymbol{\omega}_{\mathbf{pi}}$ are the principle angular velocities of molecule i, $\boldsymbol{\tau}_{\mathbf{pi}}$ are the torques on molecule i due to interactions with molecule j. The axial water thermal conductivity is then given by:

$$k_z = \frac{1}{k_B V T^2} \int_0^\infty \langle J_z(t) \cdot J_z(0) \rangle dt, \tag{5}$$

where T is the system temperature, V is the system volume, and k_B is the Boltzmann constant [15].

We can further examine the thermal conductivity of the water by integrating the components of the heat current autocorrelation function individually. From Eqn. (4), we let

$$\mathbf{J}(t) = \mathbf{M} + \mathbf{T} + \mathbf{R}, \tag{6}$$

where

$$M = \sum_i \mathbf{v_i} e_i, \tag{7}$$

$$T = \frac{1}{2}\sum_i \sum_j \mathbf{r_{ij}} \left(\mathbf{v_i} \cdot \mathbf{F_{ij}}\right), \tag{8}$$

and

$$R = \frac{1}{2}\sum_i \sum_j \mathbf{r_{ij}} \left(\omega_{\mathbf{pi}} \cdot \tau_{\mathbf{pi}}\right). \tag{9}$$

In this expression, M is the energy transfer associated with mass diffusion, T is the energy transfer associated with translational effects, and R is the energy transfer associated with rotational effects. Following Eqn. 5, the thermal conductivity in the axial direction can then be written as

$$k_z = \frac{1}{k_B V T^2}\int_0^\infty \Big[\langle M \cdot M \rangle + \langle T \cdot T \rangle + \langle R \cdot R \rangle + \langle M \cdot T \rangle + \langle T \cdot M \rangle + \langle M \cdot R \rangle + \langle R \cdot M \rangle + \langle T \cdot R \rangle + \langle R \cdot T \rangle \Big] dt. \tag{10}$$

We define the volume in Eqn. 10 to be that enclosed by the CNT using the nominal (zero temperature) tube diameter. Using this decomposed heat current vector, we can identify how each molecular transport mechanism contributes to the overall water thermal conductivity.

In Table 1 we present the variation in the water axial thermal conductivity with CNT diameter, $k_z(d)$, for water inside 0.83, 1.10 and 1.26 nm diameter CNTs and for bulk water. We decompose the total thermal conductivity into contributions from rotational energy exchange [the $\langle R \cdot R \rangle$ term in Eqn. (10)] and contributions from mass diffusion (the $\langle M \cdot M \rangle$ term). We find that contributions arising from the other energy exchange mechanisms are negligible. The magnitude of the axial thermal conductivity decreases with decreasing CNT diameter, a result we attribute to confinement-induced changes in the water structure [16]. For bulk water, 98 percent of the energy transferred between molecules occurs *via* rotational energy exchange. For water inside CNTs, energy exchange is still dominated by rotational energy transfer, however, the relative contribution to energy exchange arising from mass diffusion become more important as the diameter decreases.

We find that both the structure and the vibrational spectra of water molecules inside the CNT are unaffected by the movement of the carbon atoms, suggesting that the water thermal conductivity predictions for systems with fixed carbon atoms are transferable to the composite systems investigated here. Because the CNT is fixed in space, the instantaneous system momentum is non-zero. The time-averaged system momentum, however, is zero and fluctuates with a characteristic frequency on the order of 1 ns. Since the per-molecule magnitude of the system instantaneous momentum is three orders of magnitude smaller than the molecular thermal momentum, we suspect that the contributions to the heat flux vector arising from the non-zero instantaneous momentum will be negligible. We are continuing to examine how this low-frequency motion affects thermal transport [17].

Table 1. TOTAL THERMAL CONDUCTIVITY, k_z, ROTATIONAL CONTRIBUTION TO THERMAL CONDUCTIVITY, k_{RR}, AND DIFFUSION CONTRIBUTION TO CONDUCTIVITY, k_{MM}, FOR WATER INSIDE CNTS. CONTRIBUTIONS TO THE THERMAL CONDUCTIVITY FROM OTHER TRANSPORT MECHANISMS ARE NEGLIGIBLE. ALL CONDUCTIVITIES ARE GIVEN IN W/M-K.

CNT Diameter (nm)	k_z	k_{RR}	k_{MM}
0.83	0.11	0.08	0.03
1.10	0.40	0.38	0.02
1.26	0.45	0.44	0.01
Bulk Water	0.48	0.47	0.01

THERMAL CONDUCTIVITY OF WATER/CNT COMPOSITE SYSTEMS

We predict the thermal conductivity of water/CNT composite systems using the heat flux method used to predict the thermal conductivity of hollow CNTs. After the equilibration period of 5 ns, we find that the axial temperature profiles in the CNT and in the water are identical. This condition is expected and implies that there is no net energy transfer in the radial direction between the materials.

Since an axial temperature gradient is present in both the CNT and the water, thermal energy will be transferred from the hot reservoir to the cold reservoir through both materials. Because the thermal conductivity (and corresponding thermal conductance) of the water is three to four orders-of-magnitude smaller than that of the CNT, however, a negligible fraction of the total thermal transport through the composite occurs through the water. This relationship implies that changes in the composite thermal conductivity are primarily governed by changes in phonon transport through the CNT due to interactions with the water molecules. Understanding how the water inside the CNT changes phonon transport through the tube is the key to understanding thermal transport in water/CNT systems.

In Fig. (3) we compare the thermal conductivity of water-filled CNTs to empty CNTs. Several trends are immediately apparent: First, the thermal conductivity of a water-filled CNT is

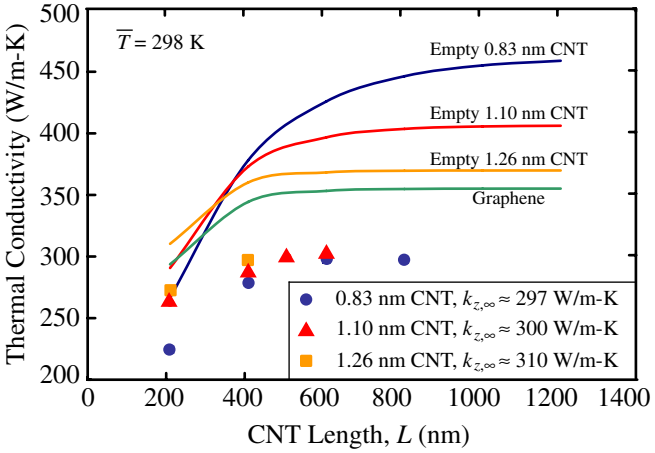

Figure 3. VARIATION IN THE THERMAL CONDUCTIVITY WITH LENGTH AND DIAMETER FOR WATER-FILLED CNTS (POINTS) AND EMPTY CNTS (LINES).

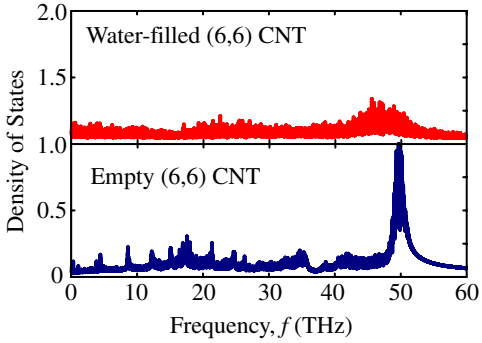

Figure 4. VARIATION IN THE CARBON ATOM DENSITY OF STATES (DOS) FOR A HOLLOW AND WATER-FILLED 0.83 NM DIAMETER 500 NM LONG CNT.

20 to 35 percent lower than the thermal conductivity of an empty CNT. Second, unlike empty CNTs, where the fully-diffusive thermal conductivity decreases with increasing diameter, the fully-diffusive thermal conductivities of the water-filled 1.26 nm, 1.10 nm, and 0.83 nm diameter CNTs are of comparable magnitude. Third, compared to empty CNTs, the transition to fully-diffusive thermal transport with increasing system length occurs for shorter CNT/water systems. This point is especially evident in the 0.83 nm CNT, where fitting the available data to Eqn. 2 gives $k_{z,99}$ =680 nm for the water filled CNT compared to $k_{z,99}$ =1090 nm for the empty CNT. We are currently performing simulations of longer 1.26 nm and 1.10 nm diameter systems.

To understand the mechanisms responsible for this behavior, we present in Fig. (4) the variation in the carbon atom phonon density of states (DOS) for both filled and hollow CNTs. The DOS describes the vibrational modes available to atoms in the CNT and is predicted in MD simulation from the Fourier transform of the velocity autocorrelation function [18]. The DOS for the hollow CNT has a maximum at 50 THz, corresponding to high-frequency vibrations of carbon atom bonds, and numerous other distinct peaks. For water-filled CNTs, however, the peaks in the DOS are less distinct. The maximum in the DOS is shifted to lower frequencies and is broadened. This behavior suggests that interactions with the water molecules dampen the vibrations within in the CNT. We are currently calculating the phonon dispersion curves of the hollow and water-filled CNT to validate this hypothesis.

SUMMARY

The effective thermal conductivity of water/CNT composite systems is predicted using MD simulation. By imposing a heat flux in the CNTs, we examined the transition to diffusive phonon transport. The length required to transition from ballistic to diffusive transport was observed to increase with decreasing nanotube diameter. The thermal conductivity of water filled CNTs is 20 to 35 percent lower than hollow CNTs, a result we attribute to changes in the phonon transport through the CNT. We are currently exploring how confinement induced changes to the water structure change its thermal conductivity. We are also examining how the CNT dispersion curves are affected by interactions with water.

ACKNOWLEDGEMENTS

This work was supported by an NSF Graduate Research Fellowship (JAT) and the Berkman Faculty Development Fund. We thank Eric Landry and Joe Turney at Carnegie Mellon University for helpful discussions.

REFERENCES

[1] Balandin, A. A., Ghosh, S., Bao, W., Calizo, I., Teweldebrhan, D., Miao, F., and Lau, C. N., 2009. "Superior thermal conductivity of single-layer graphene". *Nano Letters*, **8**, pp. 902–707.

[2] Padgett, C. W., and Brenner, D. W., 2004. "Influence of chemisorption on the thermal conductivity of single-wall carbon nanotubes". *Nano Letters*, **4**, pp. 1051–1053.

[3] Mingo, N., and Broido, D. A., 2005. "Carbon nanotube ballistic thermal conductance and its limits". *Physical Review Letters*, **95**, p. 096105.

[4] Shiomi, J., and Maruyama, S., 2008. "Diffusive-ballistic heat conduction of carbon nanotubes and nanographene ribbons". *International Journal of Thermophysics*. DOI: 10.1007/s10765-008-0516-8.

[5] Brenner, D. W., Shenderova, O. A., Harrison, J. A., Stuart, S. J., Ni, B., and Sinnott, S. B., 2002. "A second-generation reactive empirical bond order (REBO) potential

energy expression for hydrocarbons". *Journal of Physics: Condensed Matter*, **14**, pp. 783–802.

[6] Abascal, J. L. F., and Vega, C., 2005. "A general purpose model for the condensed phases of water: TIP4P/2005". *Journal of Chemical Physics*, **123**, p. 234505.

[7] Werder, T., Walther, J. H., Jaffe, R. L., Halicioglu, T., and Koumoutsakos, P., 2003. "On the Water-Carbon Interaction for Use in Molecular Dynamics Simulations of Graphite and Carbon Nanotubes". *Journal of Physical Chemistry B*, **107**, pp. 1345–1352.

[8] Allen, M. P., and Tildesley, D. J., 1987. *Computer Simulation of Liquids*. Clarendon Press, Oxford.

[9] Thomas, J. A., and McGaughey, A. J. H., 2008. "Density, distribution, and orientation of water molecules inside and outside carbon nanotubes". *Journal of Chemical Physics*, **128**, p. 084715.

[10] Thomas, J. A., and McGaughey, A. J. H., 2008. "Reassessing Fast Water Transport Through Carbon Nanotubes". *Nano Letters*, **9**, pp. 2788–2793.

[11] Thomas, J. A., and McGaughey, A. J. H., 2009. "Water Flow in Carbon Nanotubes: Transition to Subcontinuum Transport". *Physical Review Letters*, **102**, p. 184502.

[12] Ikeshoji, T., and Hafskjold, B., 1994. "Non-equilibrium molecular dynamics calculation of heat conduction in liquid and through liquid-gas interface". *Molecular Physics*, **81**, pp. 251–261.

[13] Lukes, J. R., and Zhong, H., 2007. "Thermal conductivity of individual single-wall carbon nanotubes". *Journal of Heat Transfer*, **129**, pp. 705–716.

[14] Evans, D. J., and Murad, S., 1989. "Thermal conductivity in molecular fluids". *Molecular Physics*, **68**, pp. 1219–1223.

[15] Landry, E. S., Hussein, M. I., and McGaughey, A. J. H., 2008. "Complex superlattice unit cell designs for reduced thermal conductivity". *Physical Review B*, **77**, p. 184302.

[16] Alexiadis, A., and Kassinos, S., 2008. "Molecular Simulation of Water in Carbon Nanotubes". *Chemical Reviews*, **108**, pp. 5014–5034.

[17] Eapen, J., Li, J., and Yi, S., 2007. "Mechanism of Thermal Transport in Dilute Nanocolloids". *Physical Review Letters*, **98**, p. 028302.

[18] Dove, M. T., 1993. *Introduction to Lattice Dynamics*. Cambridge, Cambridge.